International Journal of Pharmaceutics 500 (2016) 144–153

Contents lists available at ScienceDirect

International Journal of Pharmaceutics

journal homepage: www.elsevier.com/locate/ijpharm

Development of TMTP-1 targeted designer biopolymers for gene delivery to prostate cancer

John W. McBride[a], Ashley S. Massey[a], J. McCaffrey[a], Cian M. McCrudden[a], Jonathan A. Coulter[a], Nicholas J. Dunne[b], Tracy Robson[a], Helen O. McCarthy[a,*]

[a] School of Pharmacy, Queen's University Belfast, 97 Lisburn Road, Belfast BT9 7BL, Northern Ireland, UK
[b] School of Mechanical and Aerospace Engineering, Queen's University Belfast, Stranmillis Road, Belfast BT9 5AH, UK

ARTICLE INFO

Article history:
Received 12 November 2015
Received in revised form 13 January 2016
Accepted 14 January 2016
Available online 21 January 2016

Keywords:
Biopolymer
Delivery system
Nanoparticles
Gene Therapy
TMTP-1

ABSTRACT

Designer biopolymers (DBPs) represent state of the art genetically engineered biomacromolecules designed to condense plasmid DNA, and overcome intra- and extra- cellular barriers to gene delivery. Three DBPs were synthesized, each with the tumor molecular targeting peptide-1 (TMTP-1) motif to specifically target metastases. Each DBP was complexed with a pEGFP-N1 reporter plasmid to permit physiochemical and biological assay analysis. Results indicated that two of the biopolymers (RMHT and RM_3GT) effectively condensed pEGFP-N1 into cationic nanoparticles <100 nm and were capable of transfecting PC-3 metastatic prostate cancer cells. Conversely the anionic RMGT DBP nanoparticles could not transfect PC-3 cells. RMHT and RM_3GT nanoparticles were stable in the presence of serum and protected the cargo from degradation. Additionally it was concluded that cell viability could recover post-transfection with these DBPs, which were less toxic than the commercially available transfection reagent Lipofectamine® 2000. With both DBPs, a higher transfection efficacy was observed in PC-3 cells than in the moderately metastatic, DU145, and normal, PNT2-C2, cell lines. Blocking of the TMTP-1 receptors inhibited gene transfer indicating internalization via this receptor. In conclusion RMHT and RM_3GT are fully functional DBPs that address major obstacles to gene delivery and target metastatic cells expressing the TMTP-1 receptor.

1. Introduction

It has long been anticipated that gene therapy will become a revolutionary technology for the treatment of metastatic cancers. However, in order to meet this expectation, innovative delivery systems are required. These gene delivery systems must protect the cargo, overcome an array of intra- and extra- cellular barriers, confer a targeting capability, release the cargo and have a limited inherent toxicity (McCrudden and McCarthy, 2013).

Various gene delivery strategies overcome many of these hurdles and have therefore emerged to prominence in the field, however they each have inherent limitations. Viral vectors exhibit immunogenicity and toxicity concerns, lipoplexes have reproducibility issues and toxicity concerns, and polyplexes have problematic biocompatibilities and low transfection efficacies (Pack et al., 2005; Zhang et al., 2012). An appealing alternative utilizes biomimetics that are capable of interacting and shuttling nucleic acids in tunable and targeted virus-like nanoparticles (Unzueta et al., 2014). Protein based biomimetics are of particular interest as they are fully biocompatible and biodegradable. Furthermore protein based vectors are customizable due to the broad spectrum of moieties available for synthesis (Seow and George, 2011).

One such platform involves genetically engineering highly cationic biopolymers with tandem repeating units through an *Escherichia coli* expression system (Hatefi et al., 2006). This manufacturing process utilizes a one-step genetic engineering approach and permits the design of vector architecture at the molecular level. The method removes the necessity for numerous conjugation/purification steps, consequently reducing the complexity of synthesis (Karjoo et al., 2013). Numerous intricate non-viral gene delivery systems, namely Designer Biopolymers (DBPs), have been developed using genetic engineering technology (Canine et al., 2011; McCarthy et al., 2011; Wang et al., 2009). DBPs are based on a one-domain-one-function concept, with each bio-inspired peptide domain working in concert to successfully deliver nucleic acids to a target cell population. It has previously been demonstrated that DBPs form spontaneously self-assembling nanoplexes with plasmid DNA (pDNA), exhibit a low-toxicity, and

* Corresponding author. Fax: +44 2890 247794.
E-mail address: h.mccarthy@qub.ac.uk (H.O. McCarthy).

http://dx.doi.org/10.1016/j.ijpharm.2016.01.039
0378-5173/

specifically target cell lines of interest. Cell lines that have been targeted include ZR-75-1 breast cancer cells and SK-OV-3Her2-positive ovarian cancer cells (Canine et al., 2011; Wang et al., 2009). In addition DBPs have mediated efficient gene transfer of suicide genes, including inducible nitric oxide synthase (iNOS), thymidine kinase (TK) and tumour necrosis factor-related apoptosis-inducing ligands (TRAIL), to these aforementioned cancer cell lines (Mangipudi et al., 2009; McCarthy et al., 2011; Wang et al., 2009).

Despite progress in molecular therapeutics the majority of cancer-related mortalities are the consequence of distant metastases rather than the primary tumors. For example, there are over 40,000 men diagnosed annually with prostate cancer (PCa) in the United Kingdom (UK), of which a third develop a metastatic and castration-resistant prostate cancer (mCRPC) with an associated survival<19 months (Cancer Research, 2015; Prostate Caner, 2015). For these patients the outlook is poor because CRPC tumours are both radio- and chemo- resistant, exhibit a distinct bone tropism with treatment options that are mainly palliative. Therefore there is a desperate unmet need for alternative gene delivery vehicles capable of systemically targeting CRPC.

Herein, we report on three DBPs for targeted gene transfer to metastatic PCa, principally examining their physiochemical characteristics and activity in a range of metastatic PCa cell lines. Each platform; RMGT, RM_3GT, and RMHT (Fig. 1), was genetically engineered and contains moieties to overcome specific barriers to gene delivery. Each DBP has a nuclear localization signal (NLS) known as R, a DNA condensing motif (DCM) known as M, an endosomal disruption motif (EDM) known as G, and a targeting peptide (TP) known as T for site specificity. The rationale for examining multiple DBPs is that certain moieties could behave somewhat unpredictably and interfere with the three-dimensional functionality of a vector, impacting upon specific gene transfer efficiency.

The NLS, DCM, and TP sequences are identical for each DBP and could be considered the base of each vector. The NLS, *Rev*, sequence was adopted from the human immunodeficiency virus type-1 and facilitates microtubule-assisted transport to the nucleus (Cochrane et al., 1990). The highly cationic DCM, μ peptide was derived from the adenovirus and invokes charge-charge interactions with DNA resulting in encapsulation into 80–110 nm-sized particles (Keller et al., 2002). The TP, tumor molecular targeting peptide-1 (TMTP-1), was identified using the FliTrx bacterial peptide display system and binds to highly metastatic tumour cell lines with an affinity for micro-metastases (Yang et al., 2008).

In addition RMGT and RM_3GT are equipped with GALA, a pH-dependent amphipathic EDM, which facilitates endosomal escape (Nicol and Szoka, 2004). RM_3GT contains three repeating units of μ as it was speculated that GALA's anionic nature might reduce the overall charge of the nanoplex and prevent efficient gene transfer. Finally the EDM in RMHT is a pH-sensitive histidine-rich fusogenic H5WYG peptide derived from the N-terminal segment of the HA-2 subunit of the influenza virus. H5WYG confers endosomal disruption upon protonation of the histidyl imidazole rings interspersed throughout its sequence (Midoux et al., 1998).

We hypothesize that the DBPs multiple functional domains will condense pDNA into non-toxic nanoparticles, protect DNA from serum endonuclease directed degradation, target metastatic PCa, internalize via receptor-mediated endocytosis, disrupt endosomal

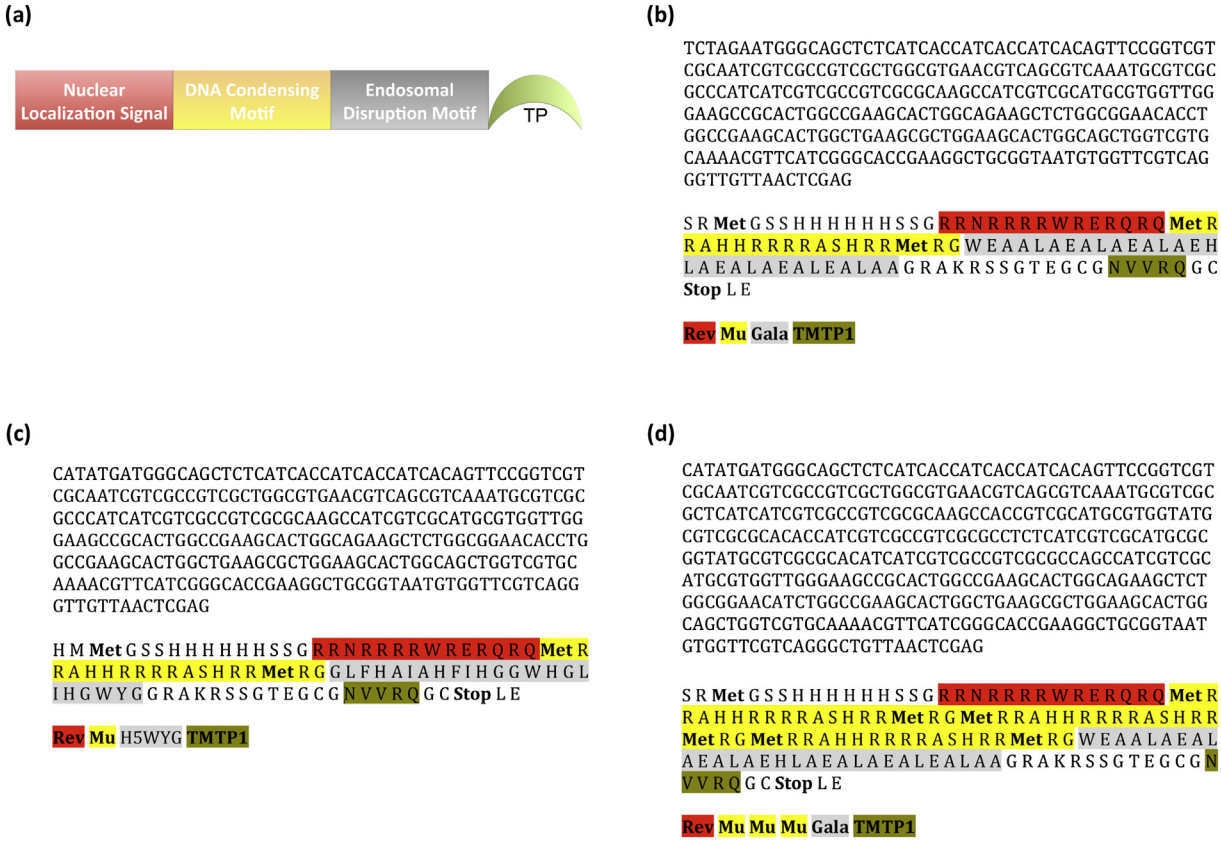

Fig. 1. (a) Schematic representation of the designer biopolymers (DBPs) (b) RMGT, (c) RMHT, and (d) RM_3GT. Each DBP is composed of a DNA condensing motif (DCM) to condense plasmid DNA—yellow, a TMTP-1 targeting peptide (TP) for specificity—green, an endosomal disruption motif (EDM)—grey, and a nuclear localisation signal motif (NLS)—red. A spacer sequence to confer flexibility was also incorporated before the TMTP-1. (For interpretation of the references to colour in this figure legend, the reader is referred to the web version of this article.)

membranes, and exploit nuclear translocation via microtubules to mediate gene expression.

2. Materials and methods

2.1. Materials and cell lines

RMHT, RMGT, and RM_3GT encoding nucleic acid sequences were synthesized and subcloned, by Genscript (NJ, USA), into a pET21b (+) expression vector (Merck, UK) under control of a T7 promoter. *E. coli* BL21(DE3) pLysS competent cells were purchased from Novagen, UK, and Circlegrow from MP Biomedical, UK. Isopropyl β-D-1-thiogalactopyranoside (IPTG), Na_2HPO_4, Guanidine HCl, imidazole, glycrol, bis-tris propane, sodium chloride, ethidium bromide, Triton-X and sodium dodecyl sulphate (SDS) were procured from Sigma–Aldrich, UK. Tris–HCl, 10% Bis-Tris gels and SeeBlue Plus2 Pre-stained Standard for SDS-PAGE, 1 Kb Plus DNA ladder, and Lipofectamine 2000 were purchased from Invitrogen, UK. The reagents for confocal microscopy; Hoechst nuclear stain, Fluorescein (FITC)-phalloidin and ProLong Gold Antifade Reagent were purchased from Life Technologies, UK, apart from the Cy-3 fluorophore which was obtained from Mirus, USA. Protease inhibitor cocktail 7 was supplied by Calbiochem, UK, EDTA free protease inhibitor tablets and WST-1 reagent from Roche, UK, Ni-NTA resin from Qiagen, UK, Sephadex G25 medium from GE Healthcare, UK, Bio-Rad Assay Reagent from BioRad, USA, and Agarose from Bioline, UK.

PC-3 and DU145 prostate cancer cells were purchases from American Type Culture Collection (ATCC) (Manassa, VA) whereas PNT2-C2 cells were kindly donated by Prof Norman Maitland at the University of York. Cells were maintained as monolayers in Roswell Park Memorial institute (RPMI) medium (Invitrogen, UK), 10% foetal calf serum (PAA, UK), at 37 °C, 5% CO_2.

2.2. Production of recombinant DBPs

The expression vectors were transformed into BL21(DE3) pLysS competent cells (Novagen, UK) as per the manufacturer's instructions. Each vector contained a hexahistidine tag to facilitate Ni-NTA agarose affinity chromatography. 200 ml starter cultures, containing 50 μg/ml ampicillin, were grown in LB media overnight at 37 °C. The LB was used to inoculate 1 L of Circlegrow medium, containing 50 μg/ml ampicillin, and incubated in an orbital shaker at 30 °C until the absorbance reached 0.8–1.2 (600 nm). Subsequently 0.4 mM (IPTG) was added to induce protein expression. After 6 h cells were harvested by centrifugation at 4000 × *g* for 15 min, 4 °C, and then pellets were frozen at −20 °C until required.

The pellet was resuspended in 25 ml of lysis buffer (100 mM Na_2HPO_4, 10 mM Tris–HCl, 6 M Guanidine HCl titrated to pH 8, 150 μl protease inhibitor cocktail 7, and 1.5 EDTA free protease inhibitor tablets. A further 50 ml of lysis buffer was added to the resuspended pellet and agitated for 1 h prior to centrifugation for 1 h at 4000 × *g*. The supernatant was adjusted to 10 mM imidazole, and 1.8 ml of equilibrated Ni-NTA resin was added then rocked for 1 h at 30 rocks/min. Following centrifugation at 4000 × *g* for 3 min the supernatant was discarded and resin was loaded onto a 0.8 × 4 ml PolyPrep chromatography column (BioRad, UK) and washed with 20 ml of wash buffer consisting of lysis buffer, 10% glycerol, 0.5 EDTA free protease inhibitor tablets, and imidazole, titrated to pH 8. Various imidazole concentrations were tested to identify the binding affinity of each DBP and thus achieve optimal purification: RMGT, 20 mM; RMHT, 25 mM; and RM_3GT, 25 mM. DBPs were eluted using a buffer consisting of 4 M guanidine HCl, 10 mM Tris-HCl, and 250 mM imidazole titrated to pH 8. DBP-rich fractions were collected in 500 μL volumes. Sample purity and expression was verified using SDS-PAGE against a pre-stained protein ladder and samples were stored in 50% glycerol, −20 °C.

2.3. Desalting and quantification of DBPs

The purified protein was desalted through an equilibrated Sephadex G25 medium contained in a 10 ml polypropylene column (BioRad, USA). On the day of experiment the column was first equilibrated with 20 ml BTP buffer (10 mM bis tris propane and 5 mM sodium chloride titrated to pH 7). Then a DBP-rich fraction was added to the column and once elution ceased 5 ml BTP buffer was added. All flow through was collected as 1 ml fractions and immediately stored on ice. The concentration of the desalted solution was quantified using a Bradford assay using Bio-Rad Assay Reagent and read at 595 nm on a Nanodrop 2000 spectrophotometer (Thermoscientific, UK).

2.4. Preparation of DBP/pDNA nanoparticles

The quantity of DBP protein to μg of DNA required for a given N:P ratio (the molar ratio of nitrogen atoms in the polypeptide to negative charges of the pDNA phosphate backbone) was calculated. SDS-PAGE revealed that dimers were predominantly purified, due to disulfide bond formation between cysteine residues, and therefore the dimer molecular weight was used in all subsequent experiments. The two constituents, DNA and DBP, were mixed in water and incubated for 30 min at room temperature before use.

2.5. Gel retardation assay

A gel retardation assay was employed to analyze the ability of each DBP to neutralize the negative charge of the plasmid DNA (pEGFP-N1). Samples at a range of N:P ratios 1–10, and DNA ladder, were run on a 1% w/v agarose gel, 0.5 μg/ml ethidium bromide, for 40 min at 100 V. The gel was visualized using a UV transilluminator (UVP, USA). Resulting images are representative of three independent studies.

2.6. Particle size and charge analysis

DBP/pEGFP-N1 nanoparticles were prepared at a range of N:P ratios using 1 μg of DNA. Nanoparticles were diluted in 1 ml of molecular grade water in a polystyrene cuvette (Sarstedt, Leicester). The mean hydrodynamic particle size was determined using Dynamic Light Scattering (DLS) with the Malvern Nano Zetasizer and DTS Software (Malvern Instruments, UK). Zeta potential was analyzed using a foldable capillary cell (Sarstedt, Leicester). The data was reported as the mean ± SEM, with an $n = 3$.

2.7. Cell transfection studies

PC-3, DU145, and PNT2-C2 cell lines were seeded at cell densities of 2.25×10^4, 2.50×10^4, and 3.50×10^4 cells/well, respectively, into 96 well plates (VWR, UK). Cells were conditioned for 2 h in Opti-MEM serum free media and subsequently transfected with DBP/pEGFP-N1 at various N:P ratios, N:P 8–12 (equivalent to 1 μg of pDNA). After 4 h the media was replaced with serum supplemented culture media. Green fluorescent protein (GFP) expression was visualized using a Nikon Eclipse TE300 epifluorescent microscope (Nikon, USA) 72 h post-transfection. Green fluorescence was quantified using the FACS caliber system (BD Biosciences, UK). Data was analyzed with Cyflogic software (http://cyflogic.software.informer.com/) and fluorescent shift was calculated with 4% gating. Data was reported as mean ± SEM, $n = 3$.

2.8. Confocal microscopy

pDNA was fluorescently labeled with a Cy-3 fluorophore (Mirus, USA) per the manufacturer's instructions. PC-3 cells, 10×10^4, were seeded in a 24-well plate and incubated in serum supplemented RPMI 1640 media for 24 h. Cells were conditioned for 2 h in Opti-MEM serum free media and subsequently transfected with RMHT/cy-3-pDNA at N:P 10 (equivalent to 1 μg of pDNA). After 4 h the media was replaced with serum supplemented culture media. 48 h post transfection cells were fixed and permeabilized with 4% formaldehyde and 0.1% Triton-X for 20 min. Subsequently, cells were stained with 0.2 mg/ml Hoechst nuclear stain, and Fluorescein (FITC)-phalloidin for 15 min. Finally cells were treated with ProLong Gold Antifade Reagent. Images were captured with a TCS SP8 confocal microscope (Leica, UK) and analyzed using LAS AF Lite Software (Leica, UK).

2.9. Cell viability study

PC-3 cells, 2.25×10^4, were seeded in a 96-well plate and incubated in serum supplemented RPMI 1640 media for 24 h. Cells were conditioned for 2 h in Opti-MEM serum free media and subsequently transfected with DBP/pEGFP-N1 at N:P 10 (equivalent to 1 μg of pDNA). After 4 h the media was replaced with serum supplemented culture media. Lipofectamine 2000/pEGFP-N1 nanoparticles, 1 μg of DNA, was used as a positive control and produced per the manufacturer's instructions. Cells were incubated at 37 °C 5% CO_2, for 24 and 48 h time points before WST-1 reagent was added to each well. Following a 4 h incubation at 37 °C, the absorbance at 440 nm, was measured using an EL808 96-well plate reader (Biotek, UK). Cell viability was normalized against untreated cells that were defined as 100% viable. The data are reported as the mean of each condition ±SEM, $n = 3$.

2.10. Serum stability study

Two sets of DBP/pEGFP-N1 complexes, N:P 10, were incubated for 1 h and 6 h at 37 °C in the presence and absence of 10% fetal bovine serum. Subsequently, 10% SDS (v/v) was added, for 10 min, to one set of samples to decomplex the nanoparticles enabling analysis of DNA integrity. All samples were run for 1 h on a 1% w/v agarose gel containing 0.5 μg/ml ethidium bromide in a Tris-acetate running buffer, and visualized using a UV transilluminator (UVP, USA). A 1 Kb Plus DNA ladder was used as a marker. Image is the representative image of three independent studies.

2.11. Competitive inhibitor study

A range of free TMTP-1 peptide concentrations were first added to PC-3 cells in Opti-MEM and subsequently DBP/pEGFP-N1 complexes, N:P 10, were added as per the *Cell transfection studies*. Opti-MEM was replaced after 2 h and analysis was carried out as per *Cell transfection studies* after 48 h. Data was reported as mean ± SEM, $n = 3$.

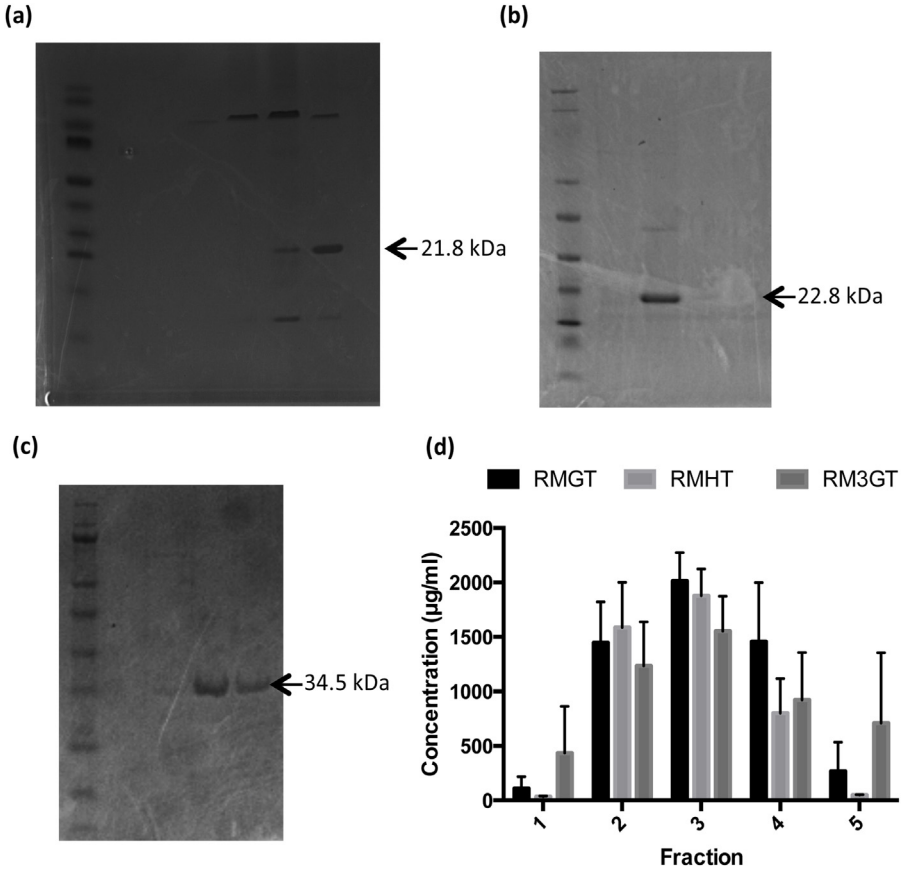

Fig. 2. SDS-PAGE of purified designer biopolymer (DBP) fractions. Samples were run at 200 V on a 10% Bis-Tris gel against a 1Kb+ ladder. (a) RMGT, washed using 20 mM imidazole, in which a 10.8 and 21.8 kDa monomer and dimer were resolved. (b) RMHT, washed with 25 mM of imidazole in which a clean 22.8 kDa dimer was eluted. (c) RM_3GT, 25 mM imidazole wash step, in which the 34.5 kDa protein was resolved (d) Protein concentration of each fraction collected, estimated using a Bradford assay. Results displayed as mean ± SEM, $n = 3$.

2.12. Statistical analysis

The statistical data for the cytotoxicity assay was generated using the one-way ANOVA Tukey post-hoc test for multiple comparisons when investigating a single time point, and the Student's*t*-test was used for toxicity comparisons of each DBP across time points. The one-way ANOVA Tukey post-hoc test was also implemented when comparing the transfection efficacy across cell lines and in the inhibitor study. Graphpad Prism (Graphpad Software 4,0, Inc., Sand Diego, CA, USA) was used for all statistical analysis.

3. Results and discussion

A model gene delivery vehicle should protect its nucleic acid cargo while specifically delivering its payload without cytotoxicity. Furthermore, for clinical application, it is extremely favorable if these vectors are cost-effective and reproducible, with a simple synthesis and purification method that is amenable to scale-up (Allen and Cullis, 2013; Lammers et al., 2012). DBP's have previously been shown to form self-assembling nanoplexes capable of targeted gene delivery coupled with low-toxicity (Canine et al., 2011; Wang et al., 2009). Additionally, the manufacturing process utilizes a one-step genetic engineering approach, which removes the necessity for numerous conjugation/purification steps, consequently reducing variability, synthesis complexity, and cost (Canine et al., 2011; Ghandehari and Hatefi, 2010; Karjoo et al., 2013).

Here, three DBPs (Fig. 1) were manufactured by recombinant engineering technology. Each DBP was comprised of four functional peptide motifs of diverse biological origin, each with a specific role in overcoming intra- and extra- cellular barriers, and was synthesized as a single chain fusion biopolymer. The base moieties were a *Rev* NLS followed by μ DCM, at the N-terminus, and a TMTP-1 TP positioned at the C-terminus. Both RMGT and RM_3GT contained the pH responsive fusogenic peptide GALA as the EDM, while the latter contained three repeating units of μ. The only difference between RMHT and RMGT is that the μ EDM was replaced with H5WYG. Each construct was characterized with a range of physicochemical and biological assays to determine their functionality and target specificity to the metastatic cancer cell line PC-3.

Each DBP was synthesized and purified using recombinant DNA technology under stringent conditions. Expression vectors that encode the his-tagged DBP sequences were transformed into BL21 (DE3) pLysS *E. coli* and vector synthesis was induced with 0.4 mM IPTG before subsequent purification via nickel bead affinity chromatography. Low concentrations of imidazole were used during the purification process to displace non-specific protein-nickel interactions. Imidazole competes for nickel binding with non-specific proteins that contain histidine, as this amino acid has imidazole functional groups. The same mechanism is exploited to

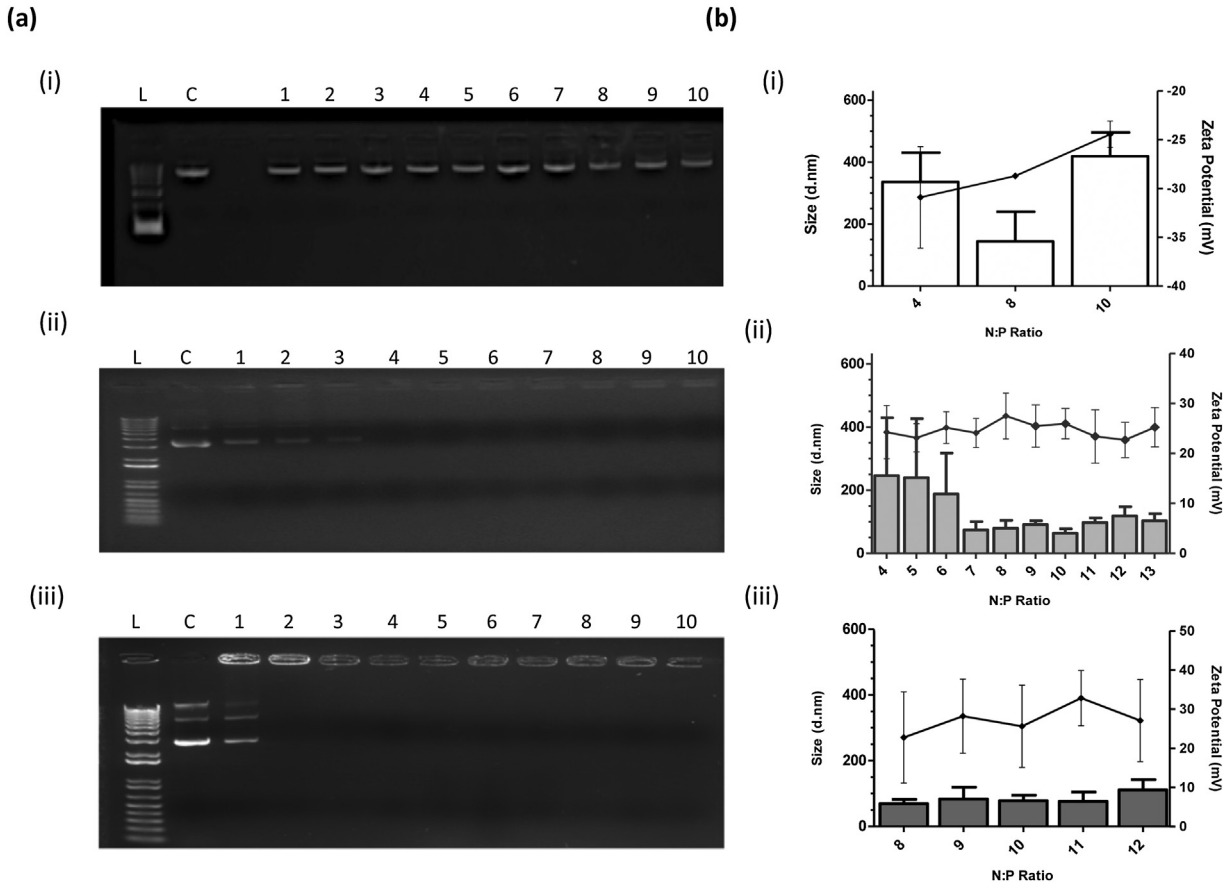

Fig. 3. (a) Agarose gel retardation assay analysing a range of designer biopolymers (DBPs) ((i) RMGT, (ii) RMHT, and (iii) RM_3GT) ability to neutralize pEGFP-N1 over a range of nitrogen (DBP): phosphate (DNA) (N:P) ratios. Nanoparticles were prepared using 1 μg DNA and incubated for 30 min before loading onto the agarose gel. L: 1 Kb Plus ladder; C: DNA only; 1–10: N:P ratios. Images representative of three independent repeats. (b) Mean hydrodynamic size and zeta potential of designer biopolymers (DBPs) ((i) RMGT, (ii) RMHT, and (iii) RM_3GT) complexed with DNA over a range of nitrogen (DBP): phosphate (DNA) (N:P) ratios. DBP nanoparticles were prepared with 1 μg of pEGFP-N1 and incubated for 30 min prior to analysis with the Malvern Zetasizer Nano. Results displayed as mean ± SEM, $n = 3$. A minimum of 15 measurements were performed for each experiment.

resolve the pure DBP, when a high concentration of imidazole is required to displace its polyhistidine-tag. Each DBP therefore has a nickel affinity threshold. Ranges of imidazole concentrations were used to identify this threshold and eliminate as much non-specific protein as feasibly possible, critically without compromising DBP yield.

Expression and purity was verified using SDS-PAGE (Fig. 2a–c). Purification of 1 L of recombinant *E. coli* produced five 500 μl aliquots of DBP protein. The greatest yield for each DBP was either in fraction 2 or 3 and commonly contained approximately 2 mg/ml (Fig. 2d). This yield is comparable to previous studies using recombinant methods (Mangipudi et al., 2009). Before characterization, DBP fractions were desalted using a Sephadex column. The removal of salt ions will reduce the possibility of salt bridge formation in between the nanoparticles and thus prevent aggregation (Karjoo et al., 2013; Nouri et al., 2013).

The ability of each DBP to condense pEGFP-N1 into nanoparticles was analyzed. A gel retardation assay was used to ascertain at which N:P ratio pDNA neutralization occurred, while dynamic light scattering was used to determine hydrodynamic particle size. The gel retardation assay revealed that RMGT did not appear to neutralize pEGFP-N1. This was not unexpected, as the number of positively and negatively charged residues within the vector will neutralize itself. Indeed, regardless of the N:P ratio

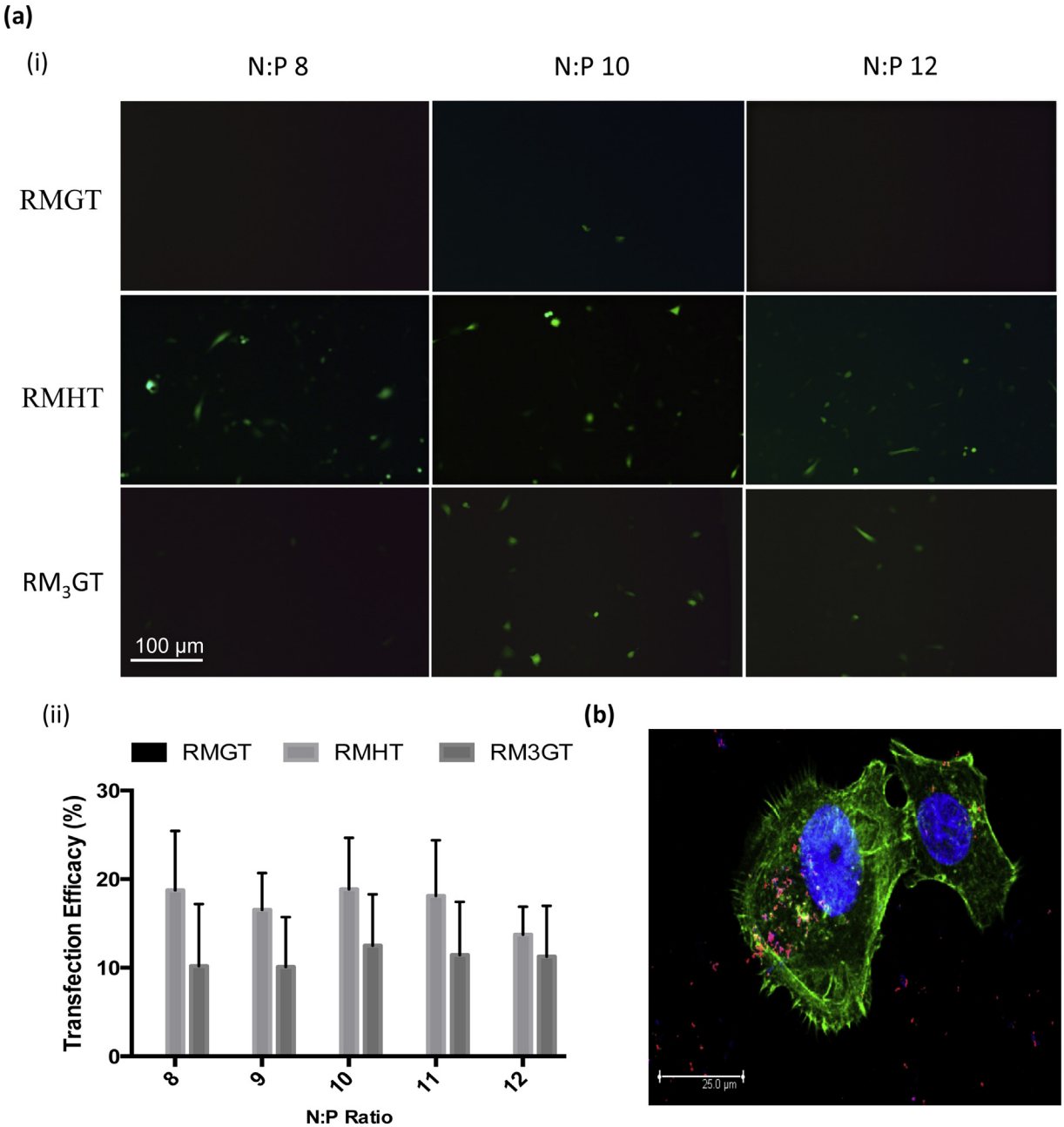

Fig. 4. (a) Evaluation of the optimal nitrogen (DBP): phosphate (DNA) (N: P) ratios for PC-3 cell transfection with the designer biopolymers (DBPs) as analyzed using (i) fluorescent microscopy and (ii) transfection efficacy 48 h post-transfection as measured by flow cytometry. Results displayed as mean ± SEM, n = 3. (b) Confocal microscopy of phalloidin stained (green—actin) and Hoechst stained (blue—nucleus) PC-3 cells transfected with RMHT:Cy-3 (red) labelledlabeled DNA. Viewed using a Leica confocal platform. (For interpretation of the references to colour in this figure legend, the reader is referred to the web version of this article.)

pDNA freely migrated down the gel, due to its negative charge, identical to the DNA only control (Fig. 3a. i). RMGT/pEGFP-N1 formed nanoparticles across a range of N:P ratios (N:P 10 hydrodynamic size of 419 ± 77 nm). However, zeta potential analysis revealed that the RMGT/pEGFP-N1 particles have an overall negative zeta potential (e.g.,–24 ± 1 mV at N:P 8) thus explaining the migration down the agarose gel (Fig. 3b. i). RMHT and RM_3GT inhibited pDNA migration, and therefore neutralized the negative charges of the phosphate backbone at N:P 4 and 2, respectively (Fig. 3a. ii–iii). RMHT/pEGFP-N1 nanoparticles exhibited a hydrodynamic diameter under 150 nm from N:P 7 and above (Fig. 3B. ii). RM_3GT formed nanoparticles under 150 nm from N:P 8 (Fig. 3. B. iii). Charge analysis revealed that the RMHT and RM_3GT nanoparticles are cationic with a surface charge of over 20 mV at a range of N:P ratios. These findings indicate that RM_3GT and RMHT formed nanoparticles via electrostatic interactions—covalent with the DNA cargo forming cationic nanoparticles.

The functionality of the DCM is to neutralize and condense DNA, leaving the other motifs to fulfill their roles. Arginine is the optimal amino acid for DNA condensation, doing so in milliseconds (Malim et al., 1989; Murray et al., 2001). The arginine rich, μ, DCM in all three DBPs aided in DNA interaction, though with varying degrees of condensation. These results indicate that DNA neutralization and nanoparticle formation can be achieved by increasing the content of cationic moieties, or by substituting anionic moieties. To elaborate, compared to RMGT, RM_3GT contained two additional tandem μ moieties and therefore 9 additional cationic arginine residues for DNA condensation. These additions have resulted in a highly positive nanoparticle surface charge with nanoparticles <100 nm in size. On the other hand, a similar result was garnered through EDM substitution of GALA, which contains seven anionic glutamic acid residues, with H5WYG, which contains no negatively charged residues.

Next the DBPs were analyzed for their ability to transfect a conventional androgen insensitive metastatic PCa cell line, PC-3. DBP/pEGFP-N1 nanoparticles were assessed at a range of N:P ratios to determine which ratio had the maximum efficacy for each formulation. Negligible GFP expression was observed with RMGT via qualitative fluorescent microscopy, while RMHT and RM_3GT successfully facilitated transgene expression (Fig. 4). Confocal microscopy demonstrates that the Cy-3 labeled DNA is delivered into the cytoplasm and the nucleus of PC-3 cells following transfection with RMHT (Fig. 4 b). It is not surprising that both RMHT and RM_3GT transfected cells as it is widely accepted that targeted cationic nanoparticles with sizes of less than 200 nm are appropriate for cellular entry via receptor-mediated endocytosis through clathrin-coated vesicles (Rejman et al., 2004). RMHT and RM_3GT transfected optimally at N:P 10 and N:P 11 respectively. RMHT facilitated the highest and most consistent gene delivery of 19% ± 3.3 at N:P 10.

Fusogenic pH-responsive EDMs are necessary to facilitate escape from the endosomal department into the cytosol. In a previous EDM functionality study, identical single chain multifunctional tripartite biopolymers were synthesized with different EDMs, it was discovered that GALA was more efficient than H5WYG (Nouri et al., 2013). The results of this study indicate that H5WYG is optimal; however, the surrounding vector sequences must be considered as diverse complex interactions may influence gene

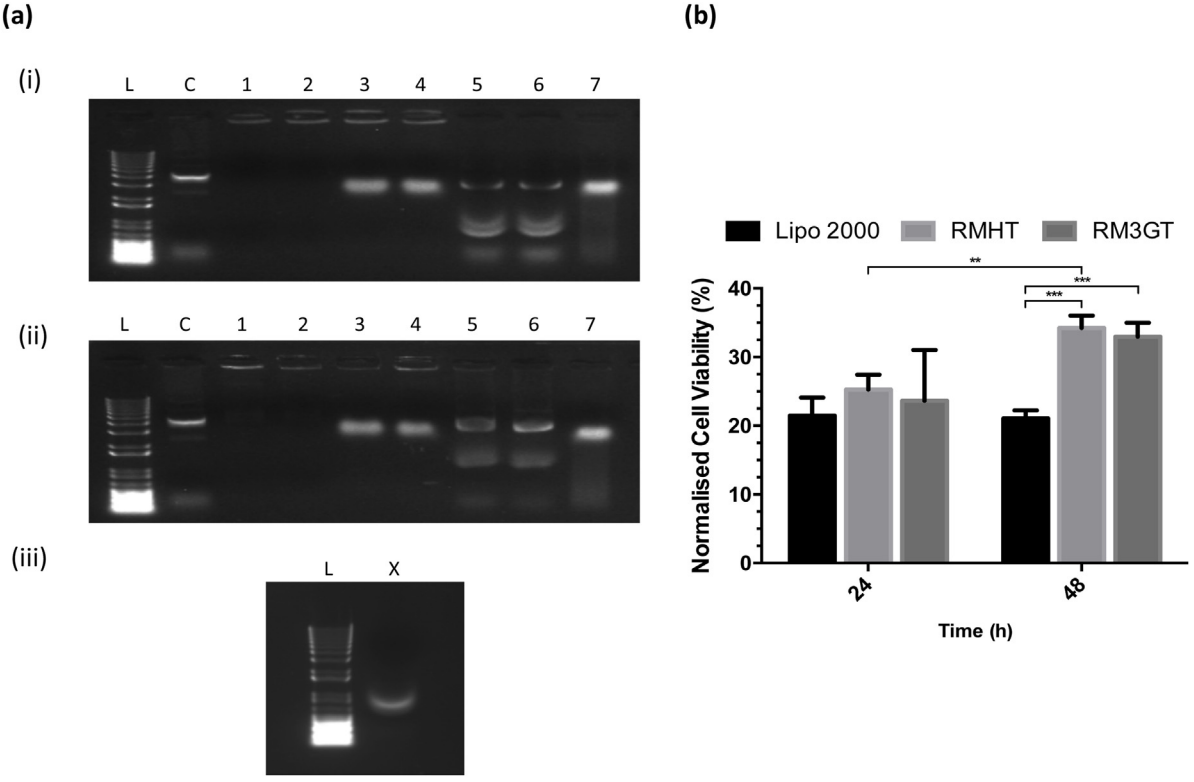

Fig. 5. Further analysis of the designer biopolymers (DBPs) RMHT and RM3GT. (a) Agarose gel illustrating the stability of (i) RMHT/pEGFP-N1 and (ii) RM3GT/pEGFP-N1 at N:P 10. Representative image of three independent experiments. L: 1Kb Plus ladder; C: DNA only; 1: DBP/DNA complexes in the absence of serum for a 1 h incubation; 2: DBP/DNA complexes in the absence of serum for a 6 h incubation; 3: DBP/DNA complexes incubated with serum for 1 h; 4: DBP/DNA complexes incubated with serum for 6 h; 5: Decomplexed DBP/DNA following 1 h incubation in serum; 6: Decomplexed DBP/DNA following 6 h incubation in serum; 7: DNA incubated with serum for 10 min. (iii) Control detailing interaction of serum incubated with SDS for 10 min. (b) Cell viability, assessed by WST-1 assay 24 and 48 h post-transfection, of PC-3 cells transfected with RMHT/pEGFP-N1 and RM3GT/pEGFP-N1, N:P 10. All results displayed as mean ± SEM, $n = 3$. $^{***}P < 0.0005$, $^{**}P < 0.01$.

transfer. For example RMHT and RM_3GT are not directly comparable with each other as the latter has additional DCMs that will impact on the overall transfection efficacy.

In the next step the optimal ratio, N:P 10, of RMHT/pEGFP-N1 and RM_3GT/pEGP-N1, for transfection were examined in a serum stability study and cytotoxicity study. A serum stability study is critical as upon intravenous administration of a nanoparticle formulation the most abundant blood plasma proteins adsorb to the surface, forming protein corona, which are replaced over time by proteins that have a higher affinity via the Vroman's effect (Vroman et al., 1980). These complex interactions can lead to pharmacokinetic complications and presentation to macrophages (Wagstaff et al., 2007). Secondly exposed pDNA is rapidly degraded by serum endonucleases so it is important that the DBPs efficiently protect their cargo.

RMHT and RM_3GT nanoparticles were stable for at least 6 h at 37 °C, in the presence of 10% serum (Fig. 5a). Furthermore when the nanoparticles were decomplexed with SDS to verify if the pDNA remained intact, the supercoiled isoform was unaltered, suggesting it was not susceptible to serum endonuclease degradation. The serum stability study also revealed that RMHT/pEGFP-N1 and RM_3GT/pEGFP-N1 nanoparticles did not interact with the serum, as a serum band is visible at 3 kb. Comparatively, after 10 min unprotected DNA exposed to serum began to degrade as demonstrated by the smear on the electrophoretic gel. The '*smile*' band at approximately 1 kb in lanes containing FCS and SDS is an interaction between the two and is not due to interaction with the pDNA or DBP (Fig. 5a. iii). This evaluation suggests that the nanoparticles are stable, and that the DBP's protect the payload from endonucleases, which is essential if it is to reach the target destination.

The cytotoxicity study revealed that both RMHT and RM_3GT DBPs impacted on PC-3 cell viability. After 24 h the toxicity profile was similar to, but not as potent as, the commercially available Lipofectamine 2000 (Fig. 5b). Many liposome formulations, for example Lipofectamine 2000, impact on cellular processes including cell cycle control, apoptosis, cellular metabolism, and contribute to cytokine production, pore formation, and cell lysis (Dokka et al., 2000; Fiszer-Kierzkowska et al., 2011; Nguyen et al., 2007). The apparent potent toxicity with RMGT and RM_3GT could be due to sequence similarities shared with antimicrobial peptides, as they are also comprised of cationic and lipophilic residues that bind to anionic cell membrane proteins subsequently reducing their integrity (Hancock, 1997; Hilchie et al., 2011). Similar to the findings here, it has been demonstrated that the H5WYG EDM in biopolymeric system reduced viability by approximately 50% in SKOV-3 cells when analyzed 24 h post-transfection and that a GALA EDM causes nominal toxicity (Nouri et al., 2013). However,

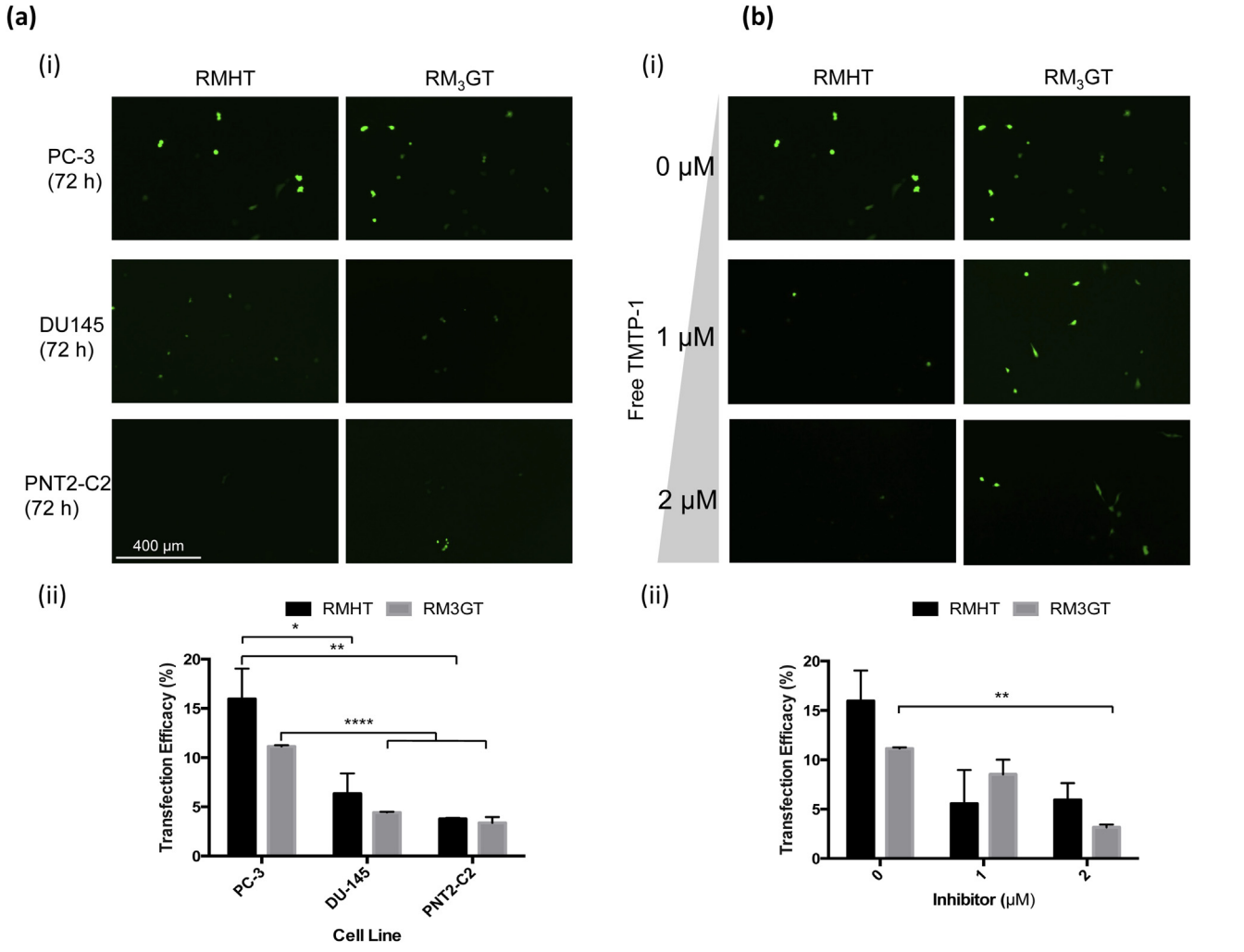

Fig. 6. Evaluation of the targeting peptide functionality of RMHT/pEGFP-N1 and RM_3GT/pEGFP-N1 at nitrogen (DBP): phosphate (DNA) (N: P) ratio 10 by (a) transfecting a range of cell lines and (b) using free targeting peptide, at various concentrations, as a competitive inhibitor. In each case (a.i–b.i) fluorescent microscopic images were captured and (a.ii–b.ii) transfection efficacy was determined via flow cytometry 48 h post-transfection. Results displayed as mean ± SEM, $n = 3$. $^{*}P < 0.05$, $^{**}P < 0.005$, $^{****}P < 0.00005$.

given the structural differences between all of these DBPs it is virtually impossible to compare one against the other, for example it has been reported that H5WYG is non-toxic as it confers a neutral charge at physiological pH, and therefore inhibits membrane interaction or internalization, ergo toxicity (Midoux et al., 1998).

Despite apparent toxicity an increase in cell viability was observed 48 h post-transfection with RMHT ($p < 0.01$) and RM_3GT, indicating cell recovery, whereas liposomal treated cells did not recover. Furthermore both biopolymers had significantly greater cell viability at 48 h compared to Lipofectamine 2000 ($p < 0.0005$). It is possible that following transfection cellular stress results in a senescence or decrease in metabolic rate before recovering to normal cell cycle (Mello de Queiroz et al., 2012). Ideally a potent, specific, and non-toxic systemic gene delivery system is required. Current nanoparticle formulations have been reported as significantly more cytotoxic than naked pDNA (Nguyen et al., 2007), though the latter is fundamentally flawed due to gene transfer inefficiency and a likelihood of degradation (Fig. 5). Here, although decreased cell viability was observed with RMHT/pEGFP-N1, N:P 10, and RM_3GT/pEGFP-N1, N:P 10, both formulations aided in transfection of PC-3 cells over pDNA, with RMHT nanoparticles exhibiting a $19\% \pm 3.3$ transfection efficacy (Fig. 4a. ii).

Targeting specificity is crucial for the application of nanomedicine to metastatic disease, as many tumors arise at inoperable distant sites. The pentamer TMTP-1 sequence has an affinity for such micro-metastasis (Yang et al., 2008). Furthermore TMTP-1 has been incorporated in polymeric systems assisting in tumor-homing imaging and targeting of anti-tumor peptides both *in vitro* and in mouse models (Li et al., 2015; Liu et al., 2012; Ma et al., 2012). To assess whether metastatic targeting was retained when the TP was included in the RMHT and RM_3GT vector design two experiments were completed. First the transfection efficacy in three PCa cell lines was examined (Fig. 6a); namely PC-3, DU145, and PNT2-C2 cells, which are highly metastatic, moderately metastatic, and a prostate normal cell line.

Selective gene transfer was observed with RMHT/pEGFP-N1 and RM_3GT/pEGFP-N1, N:P 10, as the expression in PC-3s was significantly greater than DU-145 and PNT2-C2 ($p < 0.05$). The higher transfection efficacy in PC-3 cells is most likely attributed an increase in TP ligand receptors available for internalization. A similar observation has been made with a DBP containing a HER2 targeting motif (Wang et al., 2009). Secondly, an inhibition assay was performed to demonstrate that the nanoparticles were internalized via the receptor for the TMTP-1 ligand (Fig. 6b). The exposure of free TMTP-1 to PC-3 cells had an inhibitory effect on DBP directed pEGFP-N1 delivery, with GFP fluorescence diminishing as inhibitor concentration was increased. These results suggest that the TP is functional in both vectors and utilized specific receptors to facilitate receptor-mediated endocytosis through clathrin-coated vesicles (Rejman et al., 2004). Preliminary mass spectrometry results have suggested that aminopeptidase P, a GPI-linked membrane dipeptidese vascular endothelial and lymphoid cell surface antigen, could be involved but further examination is required to confirm this (Yang et al., 2008).

4. Conclusions

The major bottleneck of gene therapy is a cost-effective, safe and efficacious delivery system. Recombinant DNA technology offers a potential solution for the production of multimeric-targeted nanomedicines in a cost effective, stable and, simple manner. Here, three systems were successfully synthesized, and have a one-dimensional design (amino acid sequence) with three-dimensional functionality. Using a reporter gene we have shown both functionality and targeting potential. If the GALA is used in these vectors, there must be a sufficient cationic charge in other motifs to compensate the anionicity. RMHT and RM_3GT formed cationic nanoparticles that specifically targeted PC-3 cells, exhibited protection from serum, all with recoverable cell viability. The functionality and molecular architecture of these DBP's warrants further investigation utilizing a cytotoxic gene to achieve therapeutic outcomes for highly metastatic prostate cancer.

Acknowledgements

This research was funded by The Mike Gooley Trailfinders Charity through Prostate Cancer UK (SO9-01).

References

Allen, T.M., Cullis, P.R., 2013. Liposomal drug delivery systems: from concept to clinical applications. Adv. Drug Deliv. Rev. 65 (1), 36–48.
Cancer Research UK, Prostate Cancer Incidence Statistics 2010 http://www.cancerresearchuk.org/cancer-info/cancerstats/types/prostate/incidence/uk-prostate-cancer-incidence-statistics (accessed 6.10.15).
Canine, B.F., Wang, Y., Ouyang, W., Hatefi, A., 2011. Development of targeted recombinant polymers that can deliver siRNA to the cytoplasm and plasmid DNA to the cell nucleus. J. Control. Release 151 (1), 95–101.
Cochrane, A.W., Perkins, A., Rosen, C.A., 1990. Identification of sequences important in the nucleolar localization of human immunodeficiency virus Rev: relevance of nucleolar localization to function. J. Virol. 64 (2), 881–885.
Dokka, S., Toledo, D., Shi, X., Castranova, V., Rojanasakul, Y., 2000. Oxygen radical-mediated pulmonary toxicity induced by some cationic liposomes. Pharm. Res. 17 (5), 521–525.
Fiszer-Kierzkowska, A., Vydra, N., Wysocka-Wycisk, A., Kronekova, Z., Jarząb, M., Lisowska, K.M., Krawczyk, Z., 2011. Liposome-based DNA carriers may induce cellular stress response and change gene expression pattern in transfected cells. BMC Mol. Biol. 12–27.
Ghandehari, H., Hatefi, A., 2010. Advances in recombinant polymers for delivery of bioactive agents. Adv. Drug Deliv. Rev. 62 (15), 1403.
Hancock, R.E., 1997. Lancet 349 (9049), 418–422.
Hatefi, A., Megeed, Z., Ghandehari, H., 2006. Recombinant polymer-protein fusion: a promising approach towards efficient and targeted gene delivery. J. Gene Med. 8 (4), 468–476.
Hilchie, A.L., Doucette, C.D., Pinto, D.M., Patrzykat, A., Douglas, S., Hoskin, D.W., 2011. Pleurocidin-family cationic antimicrobial peptides are cytolytic for breast carcinoma cells and prevent growth of tumor xenografts. Breast Cancer Res. 13 (5), R102.
Karjoo, Z., McCarthy, H.O., Patel, P., Nouri, F.S., Hatefi, A., 2013. Systematic engineering of uniform, highly efficient, targeted and shielded viral-mimetic nanoparticles. Small 9 (16), 2774–2783.
Keller, M., Tagawa, T., Preuss, M., Miller, A.D., 2002. Biophysical characterization of the DNA binding and condensing properties of adenoviral core peptide mu. Biochemistry 41 (2), 652–659.
Lammers, T., Kiessling, F., Hennink, W.E., Storm, G.J., 2012. Drug targeting to tumors: principles, pitfalls and (pre-) clinical progress. J. Control. Release 161 (2), 175–187.
Li, F., Cheng, T., Dong, Q., Wei, R., Zhang, Z., Luo, D., Ma, X., Wang, Q., Gao, Q., Ma, X., Xi, L., 2015. Evaluation of (99m)Tc-HYNIC-TMTP1 as a tumor-homing imaging agent targeting metastasis with SPECT. Nucl. Med. Biol. 42 (3), 256–262.
Liu, R., Xi, L., Luo, D., Ma, X., Yang, W., Xi, Y., Wang, H., Qian, M., Fan, L., Xia, X., Li, K., Wang, D., Zhou, J., Meng, L., Wang, S., Ma, D., 2012. Enhanced targeted anticancer effects and inhibition of tumor metastasis by the TMTP1 compound peptide TMTP1-TAT-NBD. J. Control. Release 161 (3), 893–902.
Ma, X., Xi, L., Luo, D., Liu, R., Li, S., Liu, Y., Fan, L., Ye, S., Yang, W., Yang, S., Meng, L., Zhou, J., Wang, S., Ma, D., 2012. Anti-tumor effects of the peptide TMTP1-GG-D (KLAKLAK)(2) on highly metastatic cancers. PLoS One 7 (9), e42685.
Malim, M.H., Böhnlein, S., Hauber, J., Cullen, B.R., 1989. Functional dissection of the HIV-1 Rev trans-activator–derivation of a trans-dominant repressor of Rev function. Cell 58 (1), 205–214.
Mangipudi, S.S., Canine, B.F., Wang, Y., Hatefi, A., 2009. Development of a genetically engineered biomimetic vector for targeted gene transfer to breast cancer cells. Mol. Pharm. 6, 1100–1109.
McCarthy, H.O., Zholobenko, A.V., Wang, Y., Canine, B., Robson, T., Hirst, D.G., Hatefi, A., 2011. Evaluation of a multi-functional nanocarrier for targeted breast cancer iNOS gene therapy. Int. J. Pharm. 405 (1–2), 196–202.
McCrudden, C.M., McCarthy, H.O., 2013. Cancer gene therapy–Key biological concepts in the design of multifunctional non-viral delivery systems. Gene Therap: Tools Potential Appl. 11, 213–249 Croatia, InTech.
Mello de Queiroz, F., Sánchez, A., Agarwal, J.R., Stühmer, W., Pardo, L.A., 2012. Nucleofection induces non-specific changes in the metabolic activity of transfected cells. Mol. Biol. Rep. 39 (3), 2187–2194.
Midoux, P., Kichler, A., Boutin, V., Maurizot, J.C., Monsigny, M., 1998. Membrane permeabilization and efficient gene transfer by a peptide containing several histidines. Bioconjug. Chem. 9 (97), 260–267.

Murray, K.D., Etheridge, C.J., Shah, S.I., Matthews, W., Gurling, H.M., Miller, A.D., 2001. Enhanced cationic liposome-mediated transfection using the DNA-binding peptide mu (mu) from the adenovirus core. Gene Ther. 8, 453–460.
Nguyen, L.T., Atobe, K., Barichello, J.M., Ishida, T., Kiwada, H., 2007. Biol. Complex formation with plasmid DNA increases the cytotoxicity of cationic liposomes. Biol. Pharm. Bull. 751–757.
Nouri, F.S., Wang, X., Dorrani, M., Karjoo, Z., Hatefi, A., 2013. A recombinant biopolymeric platform for reliable evaluation of the activity of pH-responsive amphiphile fusogenic peptides. Biomacromolecules 14, 2033–2040.
Pack, D.W., Hoffman, A.S., Pun, S., Stayton, P.S., 2005. Design and development of polymers for gene delivery. Nat. Rev. Drug Discov. 4 (7), 581–593.
Prostate Caner UK, About prostate cancer | Prostate Cancer UK 2013 http://prostatecanceruk.org/prostate-information/about-prostate-cancer#facts-and-figures (accessed 6.10.15).
Rejman, J., Oberle, V., Zuhorn, I.S., Hoekstra, D., 2004. Size-dependent internalization of particles via the pathways of clathrin- and caveolae-mediated endocytosis. Biochem. J. 377, 159–169.
Seow, W.Y., George, A.J.T., 2011. Peptides as promising non-viral vectors for gene therapy. In: Yuan, X. (Ed.), Non-Viral Gene Therapy. InTech, Rijeka, Croatia, pp. 616–644.
Unzueta, U., Saccardo, P., Domingo-Espín, J., Cedano, J., Conchillo-Solé, O., García-Fruitós, E., Céspedes, M.V., Corchero, J.L., Daura, X., Mangues, R., Ferrer-Miralles, N., Villaverde, A., Vázquez, E., 2014. Sheltering DNA in self-organizing, protein-only nano-shells as artificial viruses for gene delivery. Nanomed. Nanotech. Biol. Med. 10 (3), 535–541.
Vroman, L., Adams, A., Fischer, G., Munoz, P., 1980. Interaction of high molecular weight kininogen, factor XII, and fibrinogen in plasma at interfaces. Blood 55 (1), 156–159.
Wagstaff, K.M., Glover, D.J., Tremethick, D.J., Jans, D.A., 2007. Histone-mediated transduction as an efficient means for gene delivery. Mol. Ther. 4, 721–731.
Wang, Y., Mangipudi, S.S., Canine, B.F., Hatefi, A., 2009. A designer biomimetic vector with a chimeric architecture for targeted gene transfer. J. Control. Release 137 (1), 46–53.
Yang, W., Luo, D., Wang, S., Wang, R., Chen, R., Liu, Y., Zhu, T., Ma, X., Liu, R., Xu, G., Meng, L., Lu, Y., Zhou, J., Ma, D., 2008. TMTP1, a novel tumor-homing peptide specifically targeting metastasis. Clin. Cancer Res. 14 (17), 5494–5502.
Zhang, Y., Satterlee, A., Huang, L., 2012. In vivo gene delivery by nonviral vectors: overcoming hurdles? Mol. Ther. 20 (7), 1298–1304.